Dalius Mazeika*, Piotr Vasiljev, Sergejus Borodinas and Ying Yang

Piezoelectric Actuator Based on Two Bending-Type Langevin Transducers

Abstract: Langevin-type piezoelectric transducers are widely used for different industrial applications such as high-accuracy positioning, ultrasonic welding, bonding, drilling, etc. Usually Langevin-type transducers operate at longitudinal mode by employing d_{33} vibrations of piezoceramic elements. A novel design of piezoelectric actuator based on two bending-type Langevin transducers is introduced. Two half-wavelength transducers are connected by a special aluminum plate. Piezoceramic rings with two-directional polarizations are used for bending oscillation excitation. An input voltage with phase shifted by $\pi/2$ on different transducers is applied. The forward and backward elliptical motion of the contact tip is controlled by changing phases of electric signals on different transducers. A numerical simulation was carried out to investigate the trajectories of contact point motion and to validate the operating principle of the actuator. Experimental prototype of the piezoelectric actuator was fabricated, and the measurements of driven tip movements and mechanical output were performed. The results of numerical and experimental analysis are discussed.

Keywords: Langevin transducer, piezoelectric actuator, bending vibrations

DOI 10.1515/ehs-2014-0030

1 Introduction

Piezoelectric actuators are widely used for high-precision positioning, micro-manipulating, micro-pumps, valves, etc. (Uchino 1997; Uchino and Giniewicz 2003). Piezoelectric actuators have several advanced features such as high resolution, short response time, compact size and good controllability (Bansevicius et al. 1988; Sashida and Kenjo 1993; Morita 2003). Compound-type piezoelectric actuators also known as Langevin transducers are widely used for high-power applications such as ultrasonic welding, cutting and drilling. Langevin transducers have the following key features: high mechanical quality factor, low impedance and good clamping possibilities (Uchino 1997; Uchino and Giniewicz 2003; Zhao 2011). A typical design of the piezoelectric Langevin transducer consists of a piezoceramic stack and two metal blocks that are clamped by means of a pre-tension bolt (Spanner and Koc 2010). A Langevin transducer makes piezoceramic parts vibrate under compression stress due to stress applied by the bolt, so the acoustical contact between transducer parts is improved and the mechanical quality factor is increased. Usually, longitudinal vibrations of the transducer are excited employing d_{33} vibration mode of the piezoceramic parts when an alternating electric signal at the resonant frequency is applied.

Many different designs of Langevin-type piezoelectric actuators have been developed to date (Arnold and Muhlen 2001; Sherman and Butler 2007; Nakamura 2012; Roha and Kwon 2004). But only a few of them operate in a non-longitudinal vibration mode. There are reports about multimode oscillations of a Langevin-type transducer (Shi, Chen, and Liu 2006; Shi, Chen, and Liu 2008; Asumi et al. 2009; Chena and Shia 2007). A multimode transducer requires simultaneous excitation of two vibration modes such as, for example, the first longitudinal and second bending modes (Shi, Chen, and Liu 2006, 2008). An ultrasonic linear motor based on bending-type Langevin transducer has also been developed (Chena and Shia 2007). Bending-type vibrations of a Langevin transducer are excited using d_{33} mode of the two directional polarized piezoceramic parts; thus, high power conversion efficiency of lead zirconate titanate (PZT) is achieved. However, two different bending modes of a stator require that a bidirectional motion of the slider be obtained (Chena and Shia 2007). Therefore the motor cannot have identical mechanical characteristics in both forward and backward directions.

A new design of ultrasonic standing wave actuator based on two bending-type half-wavelength Langevin

***Corresponding author: Dalius Mazeika,** Faculty of Fundamental Sciences, Vilnius Gediminas Technical University, Vilnius, Lithuania, E-mail: Dalius.Mazeika@vgtu.lt

Piotr Vasiljev: E-mail: Piotr.Vasiljev@leu.lt, **Sergejus Borodinas:** E-mail: Sergejus.Borodinas@leu.lt, Institute for Scientific Research, Lithuanian University of Educational Sciences, Vilnius, Lithuania

Ying Yang, State Key Laboratory of Mechanics and Control of Mechanical Structure, Nanjing University of Aeronautics and Astronautics, Nanjing, China, E-mail: yingyang@nuaa.edu.cn

transducers is developed and presented in the paper. The actuator operates at the single resonant frequency, and the bidirectional motion of the contact tip is controlled by changing phases of electric signals on different transducers. The operating principle of the actuator is derived, and the results of a numerical simulation based on finite element modeling (FEM) are presented. A prototype actuator was fabricated and a special testing stand was developed for the experimental study. The operating principle and performance of the actuator were validated experimentally. Finally, the results of numerical simulation and experimental study are analyzed and discussed.

2 Design concept of the actuator

The actuator consists of the following parts: two half-wavelength bending-type Langevin transducers and an aluminum plate as illustrated in Figure 1. Each Langevin transducer consists of two steel blocks, eight piezoceramic rings, ten beryllium bronze electrodes and a bolt. Steel blocks of both the transducers are rigidly joined by an intermediate link. This link is used as a holder of the actuator as well (Figure 1). A special aluminum plate with a driving tip on the top surface is used to join transducers and to drive a slider.

The piezoceramic rings with opposite polarity within each half of the rings are used to excite bending mode oscillations on each transducer. The configuration of the piezoceramic elements and excitation scheme of the electrodes is shown in Figure 2.

The piezoceramic rings of each transducer are divided into two groups with the four rings in each group. Two harmonic electric signals with the phase difference of $\pi/2$ are applied on the electrodes of the different transducers (Figure 2). The upper and lower parts of the piezoceramic rings expand and contract alternately when a harmonic voltage is applied; thus, the first bending mode of Langevin transducers is excited. The elliptical trajectory of the driving tip motion is achieved applying the aforementioned excitation scheme. The direction of elliptical motion is changed by counterchanging channels of electric signals between transducers.

Let's analyze a simplified model of the proposed actuator and assume that a straight beam connects up two transducers instead of the aluminum plate. A contacting tip is located in the middle of the beam where K is a contact point (Figure 3). The beam is excited by the equivalent external forces obtained from vibrations of Langevin transducers. The phase difference between applied forces is $\pi/2$. Bending traveling wave oscillations are excited in the beam (Zhao 2011).

Let's assume that the driving tip is stiff enough to be perpendicular to the beam contour. The trajectory of point K was analyzed. Oscillations of the beam can be expressed as follows (Rao 2010):

$$y(x) = A\sin\left(\frac{2\pi}{\lambda}x - \omega t\right), \tag{1}$$

where A, λ and ω are vibration amplitude, wavelength and angular frequency, respectively, and t is time. The displacement of point K along the x axis can be expressed as

$$\Delta x_K = h\sin(\alpha), \tag{2}$$

where h is the height of the driving tip. Angle α can be obtained as follows:

$$\alpha = \frac{\partial y}{\partial x} = A\frac{2\pi}{\lambda}\cos\left(\frac{2\pi}{\lambda}x_K - \omega t\right). \tag{3}$$

Angle α is small, therefore it can be assumed that $\sin(\alpha) \approx \alpha$ and eq. (2) can be written as follows:

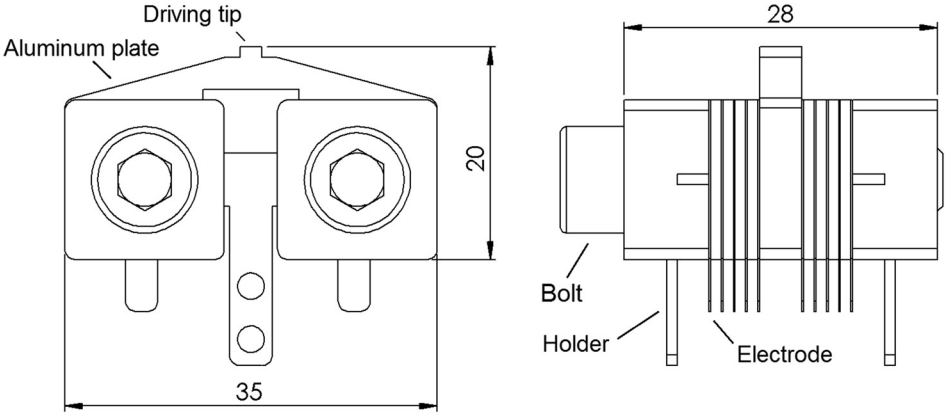

Figure 1: Design of piezoelectric actuator.

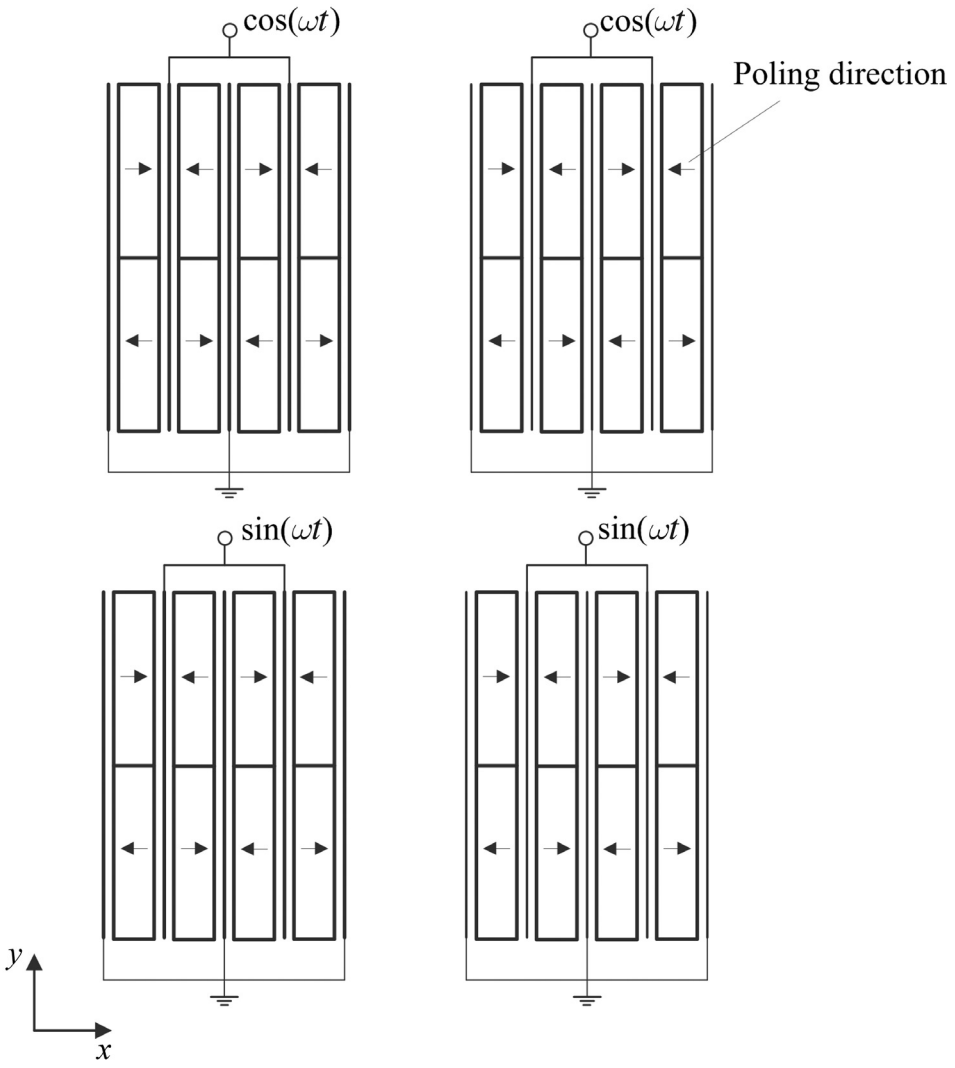

Figure 2: The configuration of the piezoceramic elements and the excitation scheme of the electrodes.

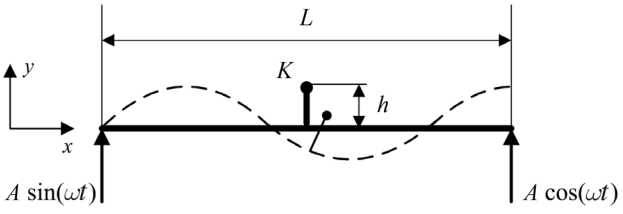

Figure 3: The principle of the actuator.

$$\Delta x_K = hA\frac{2\pi}{\lambda}\cos\left(\frac{2\pi}{\lambda}x_K - \omega t\right). \tag{4}$$

The displacement of point K along y axis can be written as

$$\Delta y_K = y(x_K) - h(1-\cos(\alpha)). \tag{5}$$

Based on the same assumption as before, it can be defined that $\cos(\alpha) \approx 1$ and eq. (5) can be written as

$$\Delta y_K = A\sin\left(\frac{2\pi}{\lambda}x_K - \omega t\right). \tag{6}$$

Taking eqs (4) and (6) together, the relation of the displacements along the x and y directions for the point K can be derived as

$$\left(\frac{\Delta x_K \lambda}{2\pi h A}\right)^2 + \left(\frac{\Delta y_K}{A}\right)^2 = 1. \tag{7}$$

Therefore the trajectory of the point K motion is an ellipse. In order to change the direction on the contact point motion, the phases of excitation voltage must be counterchanged. The proposed design of the actuator can be applied to develop high-power ultrasonic systems.

3 Numerical simulation

FEM was used to confirm and validate the operating principle of the proposed actuator. Numerical study included modal frequency analysis and harmonic response analysis. Trajectories of the driving tip were calculated. FEM software ANSYS was used to build a three-dimensional finite element model of the actuator and to run a simulation. The finite element model contains all assembling parts mentioned in the previous section except electrodes. The electrodes were not included into the model of the actuator because they significantly increase the number of the finite elements and computational time, while the changes of the accuracy of simulated results are insignificant. All parts of the actuator were bonded in the FEM model. The following materials were used in the finite element model: PZT-8 was used for modeling piezoceramic rings, steel X20Cr13 was used for the block-type parts and bolts. Properties of the materials are given in Table 1.

The actuator was rigidly clamped at the holes of the holders (Figure 1). The length of the actuator was set to 28.0 mm. The outer and inner diameter of the piezoceramic rings were 15.0 mm and 6.5 mm, respectively. The thickness of the rings was 1.0 mm. The thickness of the aluminum plate was set to 4 mm. The dimensions of the bolts were as follows: the length without the head was 28 mm, and the diameter of the bolt was 6 mm. Damping was evaluated in the model by introducing the mechanical loss factor for piezoceramic rings and the isotropic loss factor of the metallic parts. The mechanical loss factor was set to 0.004 for the piezoceramic rings and the isotropic loss factor equal to 0.001 was set for the metallic parts. Piezoelectric and dielectric losses were neglected in the model.

Modal frequency analysis of the actuator was performed. Short circuit-type electric boundary conditions were applied, i.e., a constant voltage of zero was applied at the electrodes of each piezoelectric element. While analyzing the results of resonant oscillation modes, it was determined that the oscillation mode at 33.11 kHz has dominated the first bending mode of the Langevin transducers and can be used for further investigation (Figure 4).

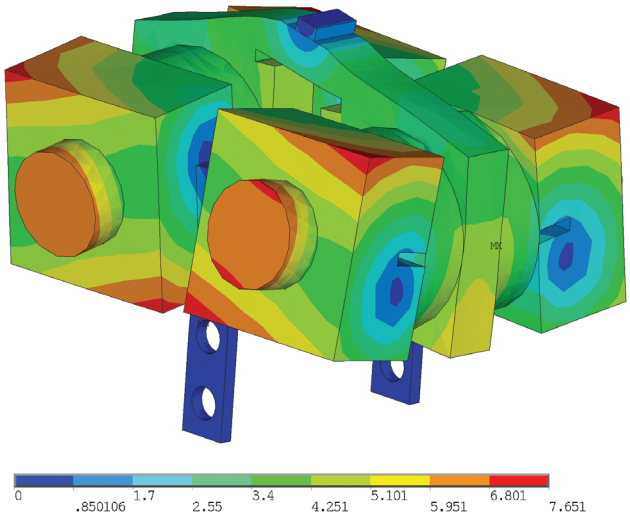

Figure 4: Modal shape of the actuator at 33.11 kHz.

Harmonic response analysis was performed with the aim to find out the actuator's response to sinusoidal voltage applied on electrodes of the piezoceramic rings and to calculate trajectories of the contact point's movement. The excitation scheme shown in Figure 2 was used during simulations. A 100 V AC signal was applied to the electrodes. A frequency range from 28 kHz to 38 kHz with a solution of 100 Hz intervals was chosen and the adequate response curves of the contact point oscillation amplitudes and phases were calculated. The results of calculations are given in Figures 5 and 6.

Graph of the contact point oscillation amplitude shows that the excitation frequency at 33.0 kHz has a local peak and is close to the natural frequency mentioned before. The 7.67 μm and 3.11 μm vibration amplitudes were obtained for displacement components u_y and u_z, respectively. Also it can be noticed that the graphs of

Table 1: Properties of the actuator materials.

Material properties	Piezoceramic PZT-8	Steel X20Cr13	Aluminum
Young's modulus [N/m^2]		2.16×10^{11}	7.0×10^{11}
Poisson's ratio		0.30	0.33
Density [kg/m^3]	7,600	7,730	2,700
Permittivity, $\times 10^{-7}$ [F/m]	$\varepsilon_{11} = 11.42$; $\varepsilon_{33} = 8.85$		
Piezoelectric matrix [C/m^2]	$e_{13} = -18.01$; $e_{33} = 29.48$; $e_{52} = 10.34$		
Elasticity matrix, $\times 10^{10}$ [N/m^2]	$c_{11} = 14.68$; $c_{12} = 8.108$; $c_{13} = 8.105$; $c_{33} = 13.17$; $c_{44} = 3.29$; $c_{66} = 3.14$		

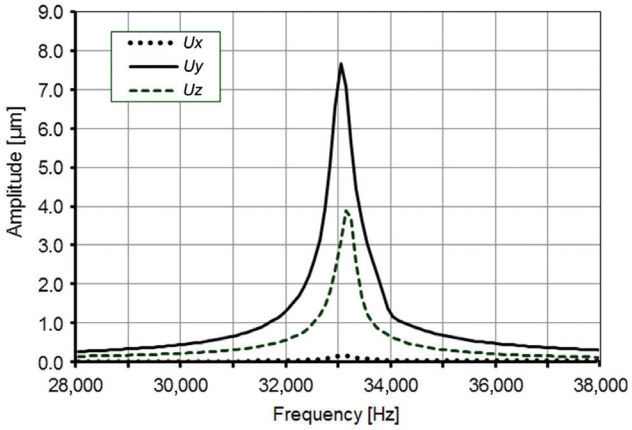

Figure 5: Simulation results: the amplitude–frequency characteristics of the contact point oscillation at two-phase excitation with $A = 100$ V.

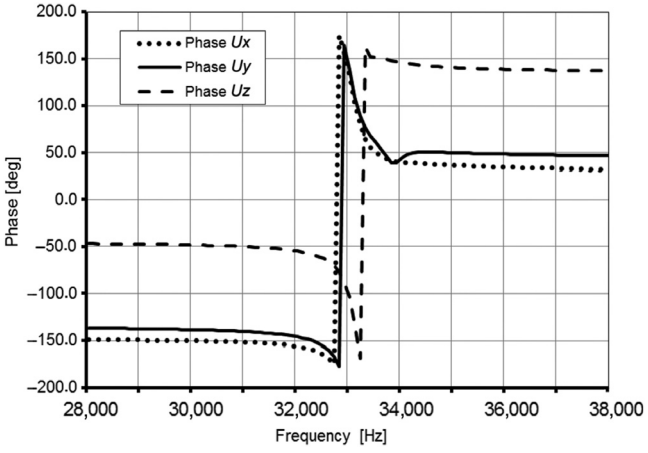

Figure 6: Simulation results: the phase–frequency characteristic of the contact point oscillation at two-phase excitation with $A = 100$ V.

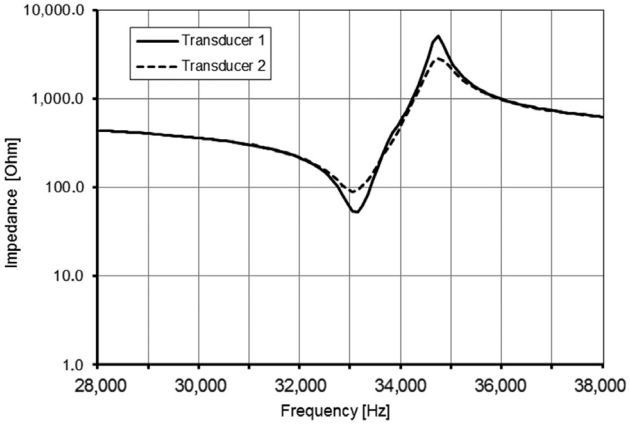

Figure 7: Impedance of the actuator versus frequency.

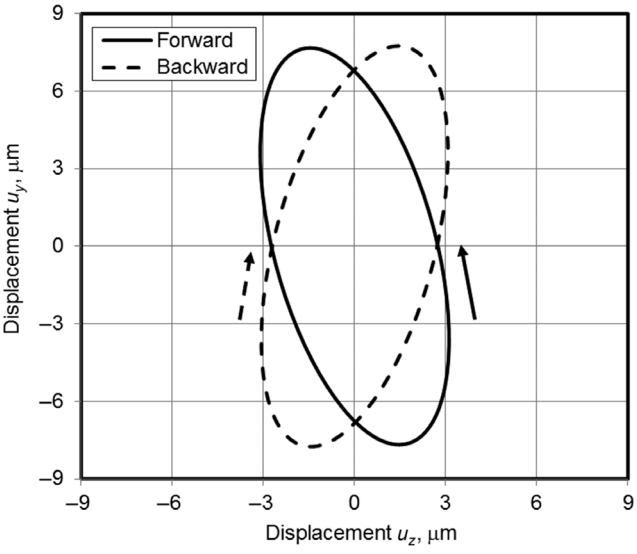

Figure 8: Simulation results: the trajectories of the contact point movement at two-phase excitation with $A = 100$ V.

the oscillation phases rapidly change at 33.0 kHz (Figure 6). This also indicates resonance oscillations of the actuator at 33.0 kHz.

The electrical impedance over a frequency range 28–38 kHz was calculated for each transducer separately (Figure 7). The impedance graphs show the resonant frequency at 33.0 kHz. It coincides with the resonant frequency value obtained from the amplitude–frequency and phase–frequency graphs presented in Figures 5 and 6.

The trajectories of the contact point motion were calculated (Figure 8). The excitation signal at 33.0 kHz was applied. Two different excitation schemes of the actuator were used for calculations, i.e., the sine–cosine scheme as shown in Figure 2 and the scheme where the phase of each signal was changed by $-\pi/2$ and $\pi/2$, respectively. While analyzing the trajectories of the contact point motion, it can be noticed that they have ellipsoidal shapes. It confirms an analytical formulation of the operating principle of the actuator. The lengths of the major and minor axes of both the ellipses are 15.6 μm and 4.1 μm, respectively. The lean angle to x coordinate axis is 100.81° and 79.4° for forward and backward motion, respectively. It must be noticed that the contact point moves in different directions when a different excitation scheme is applied. It confirms that two-directional motion of the slider will be achieved.

Based on the results of the numerical simulation it can be concluded that the operating principle of the actuator is validated. The actuator will produce bidirectional motion of the slider at the 33.0 kHz excitation frequency.

4 Experimental investigation

A prototype actuator and a special testing stand were made for the experimental study (Figure 9). A prototype actuator consists of all assembling parts described in Section 2. An alumina ceramic ball was bonded at the tip of the aluminum plate. Alumina (Al_2O_3) has good characteristics for a friction material such as high strength, hardness, wear endurance and is used to improve contact stiffness and performance of the actuator. A special stand with a linear stage was made for the experimental study. Alumina ceramic was used as a friction layer of the slider. A preload of the actuator was applied through a coil spring. The aims of the experiment were to verify results of numerical modeling, to measure the thrust force of the actuator and to find the distribution of the oscillation amplitude on the top surface of the actuator.

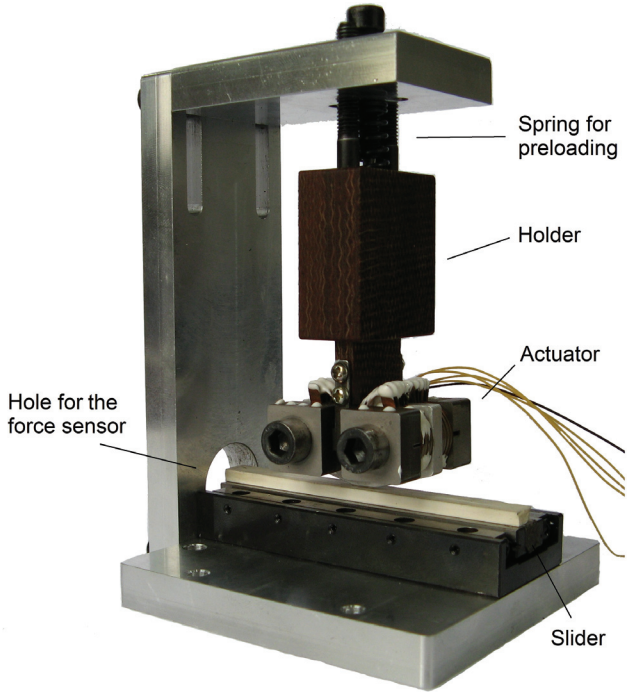

Figure 9: Prototype actuator and experimental stand.

The impedance–frequency characteristic of the actuator was measured with the help of the impedance analyzer Agilent 4294A at 10 m *V*rms. Results of the measurements are given in Figure 10. The positions of curve valleys indicate that the resonant frequencies for the first and second transducer are obtained at 30.44 kHz and 29.89 kHz, respectively. The errors between the measured and calculated frequencies mainly came from the FEM simulation, such as the inaccuracy of the material properties, neglecting of bronze electrode layers and not considering the preload force of the bolt.

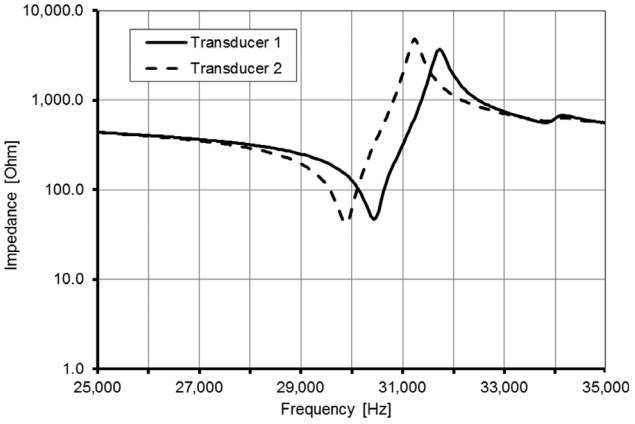

Figure 10: Measured impedance of the actuator versus frequency.

The maximum thrust force of the actuator was measured as well. The force sensor Yaohua LC1015 was used for the measurements. The sensor was fixed in the special hole of the testing stand (Figure 9). The sensor was pressed by the slider when voltage was applied to the actuator and the forward driving thrust force was measured. The actuator was turned around to measure the backward thrust force. Figure 11 shows graphs of the measured maximum output force versus the input voltage when slider is moved forward and backward. Two preload forces of the actuator were used: 15 N and 25 N. It can be noticed that the thrust force increases with the input voltage. Higher electric voltage causes larger vibration amplitude and the speed of the driving tip. The actuator achieves the maximum thrust force of 8.8 N when 25 N preload is applied and input voltage is 160 V. The weight of the actuator is 0.092 kg. This result shows that the actuator can lift about 10 times its weight.

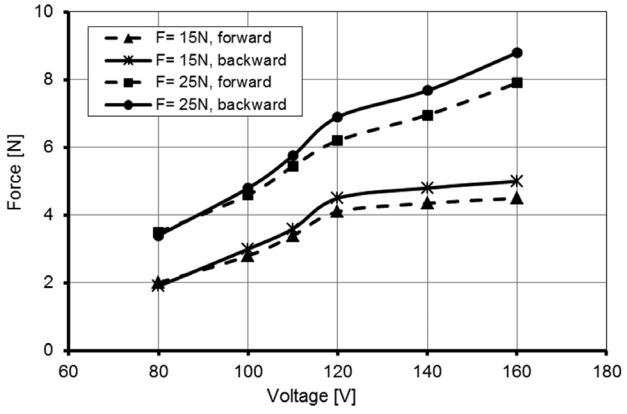

Figure 11: Maximum thrust force versus input voltage.

5 Conclusion

A novel design of a piezoelectric actuator based on two bending-type Langevin transducers was developed. An analytical model of the driving tip motion confirmed that an elliptical trajectory can be achieved using the proposed design of the actuator. Results of numerical simulation and experimental study validated the operating principle of the actuator. Bidirectional motion of the slider can be achieved by counterchanging phases of the excitation signal on the different transducers. A prototype actuator was developed and the maximum output force equal to 8.8 N was achieved.

Acknowledgment: The work was supported by the Research Council of Lithuania under project Nos. MIP-045/2014 and 111 (Grant no. B12021).

References

Arnold, F., and S. Muhlen. 2001. "The Resonance Frequencies on Mechanically Pre-Stressed Ultrasonic Piezotransducers." *Ultrasonics* 39:1–5.

Asumi, Y. K., R. Fukunaga, T. Fujimura, and M. K. Kurosawa. 2009. "High Speed, High Resolution Ultrasonic Linear Motor Using V-Shape Two Bolt-Clamped Langevin-Type Transducers." *Acoustical Science and Technology* 30(3):180–6.

Bansevicius, R., R. Barauskas, G. Kulvietis, and K. Ragulskis. 1988. *Vibromotors for Precision Microrobots*. USA: Hemisphere Publishing Corp.

Chena, W., and Sh. Shia. 2007. "A Bidirectional Standing Wave Ultrasonic Linear Motor Based on Langevin Bending Transducer." *Ferroelectrics* 350(1):102–10.

Morita, T. 2003. "Miniature Piezoelectric Motors." *Sensors and Actuators A* 103:291–300.

Nakamura, K. 2012. *Ultrasonic Transducers: Materials and Design for Sensors, Actuators and Medical Applications*. Cambridge, UK: Woodhead Publishing Ltd.

Rao, S. 2010. *Mechanical Vibrations*. Upper Saddle River, NJ: Prentice Hall.

Roha, Y., and J. Kwon. 2004. "Development of a New Standing Wave Type Ultrasonic Linear Motor." *Sensors and Actuators A* 112:196–202.

Sashida, T., and T. Kenjo. 1993. *An Introduction to Ultrasonic Motors*. Oxford: Clarendon Press.

Sherman, Ch., and J. Butler. 2007. *Transducers and Arrays for Underwater Sound*. Berlin: Springer.

Shi, Sh., W. Chen, and J. A. Liu. 2006. "High Speed Ultrasonic Linear Motor Using Longitudinal and Bending Multimode Bolt-Clamped Langevin Type Transducer." *Proc. IEEE International Conference on Mechatronics and Automation*, pp. 612–17, June 25–28. Luoyang, China.

Shi, Sh., W. Chen, J. Liu, et al. 2008. "Ultrasonic Linear Motor Using the L-B Mode Langevin Transducer with an Exponential Horn." *Frontier of Mechanical Engineering* 3(2):212–17.

Spanner, K., and B. Koc. 2010. "An Overview of Piezoelectric Motors." *Proc. Actuator* 10:167–76.

Uchino, K. 1997. *Piezoelectric Actuators and Ultrasonic Motors*. Boston, MA: Kluwer Academic Publishers.

Uchino, K., and J. Giniewicz. 2003. *Micromechatronics*. New York: Marcel Dekker Inc.

Zhao, C. 2011. *Ultrasonic Motors: Technologies and Applications*. Beijing: Science Press.